Light Well: A Tunable Free-Electron Light Source on a Chip

G. Adamo,[1] K. F. MacDonald,[1,*] Y. H. Fu,[2] C-M. Wang,[2] D. P. Tsai,[2] F. J. García de Abajo,[3] and N. I. Zheludev[1]

[1]*Optoelectronics Research Centre, University of Southampton, Southampton, SO17 1BJ, United Kingdom*
[2]*Department of Physics, National Taiwan University, Taipei 10617, Taiwan, Republic of China*
[3]*Instituto de Óptica - CSIC, Serrano 121, 28006 Madrid, Spain*

(Received 7 July 2009; revised manuscript received 17 August 2009; published 9 September 2009)

The passage of a free-electron beam through a nanohole in a periodically layered metal-dielectric structure creates a new type of tunable, nanoscale radiation source—a ''light well''. In the reported demonstration, tunable light is generated at an intensity of ~ 200 W/cm^2 as electrons with energies in the 20–40 keV range are injected into gold-silica well structures with a lateral size of just a few hundred nanometers.

DOI: 10.1103/PhysRevLett.103.113901 PACS numbers: 42.72.−g, 78.67.−n

With a view towards future highly-integrated nanophotonic devices, there is growing interest in nanoscale light and surface plasmon-polariton sources [1–5]. Electron-beam-induced radiation emission [6–8] is of particular interest because electrons can be focused to nanoscale spots (far below the diffraction limit for light), enabling such applications as high-resolution mapping of plasmonic excitations in nanostructures [9–11]. In this Letter we report on the first demonstration of *tunable* light emission from a chip-scale free-electron-driven source—a ''light well''—in which optical (visible to near-infrared) photons are generated as an electron beam travels through a nanohole in a layered metal-dielectric structure. With a lateral size of just a few hundred nanometers, and the notable advantage of wavelength tuneability, such structures may find varied application, for example, in nanophotonic circuits as on-chip light sources, or in densely packed ensembles for optical memory and field emission or surface-conduction electron-emitter displays [12].

The light well belongs to a broad family of free-electron-driven radiation sources wherein emission occurs as electrons interact with a periodically structured environment. These range from small Smith-Purcell sources [13], which emit a continuum of wavelengths over a broad angular range as electrons pass over the surface of a metal grating (with a period typically in the micro- to millimeter range), to macroscopic free-electron lasers that generate high levels of directed coherent radiation as electron pulses traverse magnetic undulators [14]. In such sources, the wavelength of emitted light can be tuned by adjusting the energy of the electron beam or the structure of the periodic surroundings. In the light well, a beam of free electrons experiences an alternating dielectric environment as it travels through a tunnel in a periodically layered metal-dielectric nanostructure and optical photons are emitted as a result. In keeping with other free-electron sources, the wavelength of radiation emitted by the light well can be tuned by adjusting the energy of the incident electrons. We report here on incoherent near-infrared emission but we anticipate that the light well concept may be developed to achieve coherent operating modes and scaled to cover a very broad range of wavelengths extending to the terahertz and ultraviolet domains.

Experimental light wells (see Fig. 1) were fabricated in a stack of eleven alternating silica and gold layers (six silica and five gold), each with a thickness of 200 nm, sputtered onto a thick gold base layer on a silicon substrate. Wells with typical diameters of around 700 nm were milled through the stack into the base layer, perpendicular to the plane of the layers, using a focused ion beam.

Characterization of the light well as an optical source was performed in a scanning electron microscope (SEM) equipped with a light-collection system comprising a small parabolic mirror positioned above the sample (collecting emitted light over approximately half of the available hemispherical solid angle and directing it out of the SEM chamber) and a spectrograph equipped with a liquid-nitrogen-cooled CCD array detector. The electron beam of the

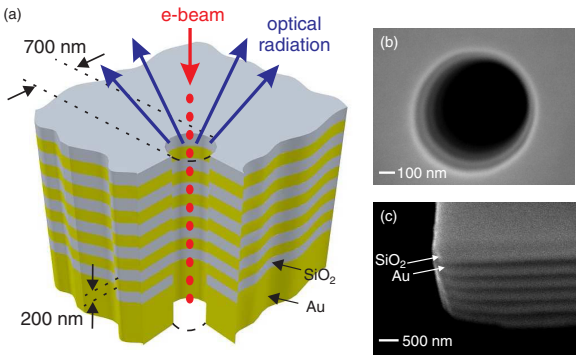

FIG. 1 (color online). (a) Schematic cut-away section of a light well, which comprises a nanohole through a stack of alternating metal and dielectric layers, into which an electron beam is launched. Light is generated as electrons travel down the well and encounter a periodic material environment. (b) Scanning electron microscope image of a light well fabricated in a gold-silica multilayer. (c) The alternating metal-dielectric layer structure as seen at an exposed corner of the sample.

SEM, focused to a spot with a diameter of ~30 nm, was used to drive light-well optical emission. Emission spectra were recorded at different acceleration voltages and beam currents (measured using a Faraday cup in the SEM column) for a number of beam injection points along the diameter of the nanohole, with reference measurements also taken for beams impacting the top (silica) surface of the multilayer outside the hole.

The following characteristic emission features have been observed: (1) When the electron beam hits the surface of the structure outside the hole, light emission is observed with a broad spectrum centered at 640 nm [Fig. 2(a)]. Within experimental accuracy this spectrum does not depend on the electron acceleration voltage and is attributed simply to cathodoluminescence and backward transition radiation from the silica-gold multilayer structure [15–17]. (2) When the electron beam is injected into the nanohole the emission spectrum contains two peaks (I and II) with spectral positions that depend on the electron acceleration voltage [Fig. 2(b)]. The emission intensity is found to increase as the injection point approaches the wall of the light well as illustrated for peak I in the inset to Fig. 2(c). (3) For a fixed injection point and electron acceleration voltage, the emission intensity increases linearly with beam current [Fig. 2(c)].

Though structurally simple, the light well's emission characteristics are controlled by a complex combination of material- and geometry-dependent processes that cannot presently be described within a single analytical or numerical model. To a first approximation, one may consider that light emission originates from an oscillating dipole source created as electrons experience a periodically modulated potential within the well. In this simplified picture, an electron passing through a metal section of the well interacts with its "mirror image," but this interaction is somewhat different in a dielectric section. This creates a monochromatic dipole of frequency $\nu = v/a$, where v is the electron velocity and a is the period of the structure, moving at the electron velocity. The radiation efficiency depends on the strength of the mirror interaction and on the density of photonic states available in the well, and therefore on its geometry and material composition as well as the proximity of electrons to the wall. In a well of finite length L, the spectral width of the emission line $\Delta\nu$ is governed by the uncertainty relation $L \times \Delta\nu \simeq v$. So, for example, with 30 keV electrons ($v \simeq c/3$) and a well length $L = 2.2$ μm (eleven 200 nm layers) one may expect an emission line with a width of ~220 nm centered at ~1200 nm, not far from what is observed in the experiment. In reality, this naïve picture is complicated by relativistic corrections, the excitation and scattering of surface plasmons on metal-dielectric interfaces within the structure, the light-guiding properties of the silica layers, and ultimately the guided-mode profile of the nanotube (see below). Nevertheless, the inverse proportionality it de-

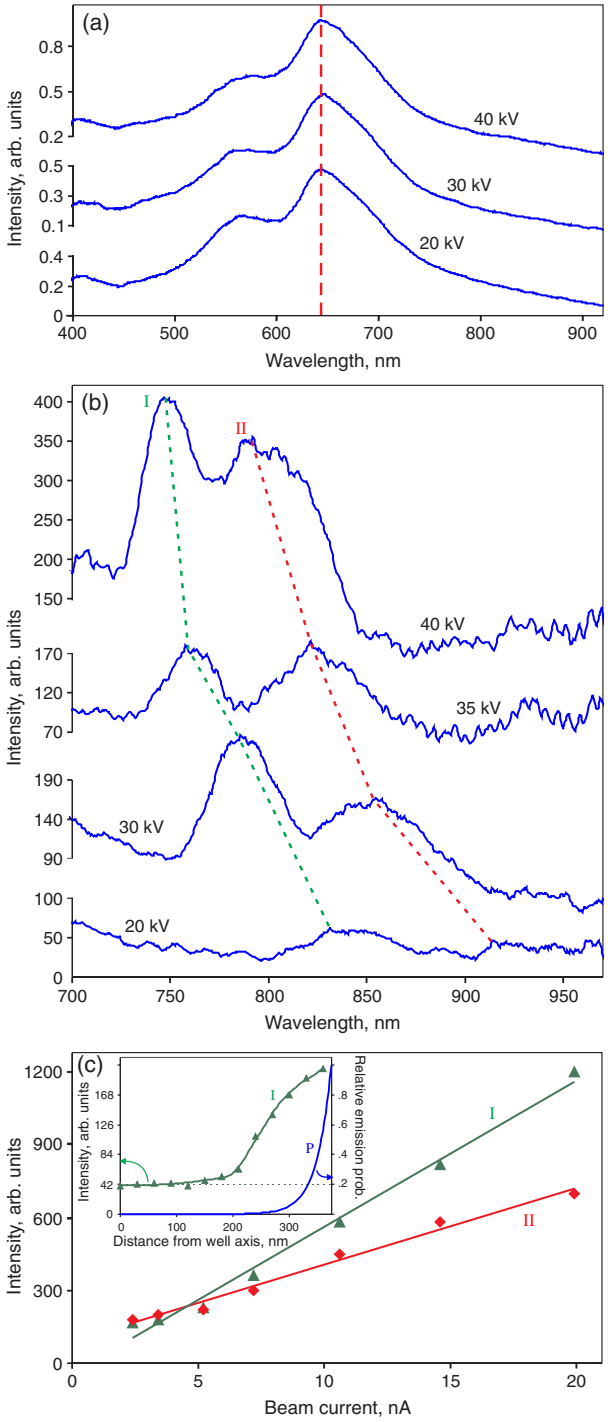

FIG. 2 (color online). (a) Emission spectra for an electron beam impact point outside the light well, i.e., on the top surface of the gold-silica multilayer, for a range of electron acceleration voltages. (b) Emission spectra for a 750 nm diameter well for acceleration voltages of 20, 30, 35, and 40 kV with a beam injection point ~100 nm inside the wall of the well. (c) Emission intensity for peaks I and II as a function of electron beam current for an acceleration voltage of 40 kV at an injection point ~100 nm inside the wall of the well. The inset shows peak I (760 nm) emission intensity at 40 kV and analytically estimated emission probability (P) as functions of beam injection position relative to the axis of a 750 nm diameter well.

scribes between emission wavelength and electron velocity is clearly seen in the blueshifting of experimentally observed emission peaks with increasing electron energy [Fig. 2(b)]. For a well of ideal cylindrical symmetry, the mirror interaction strength will be at a minimum for electrons traveling along the axis of the well and will increase with proximity to the wall, increasing the emission intensity as described above and illustrated (from experiment) in the inset to Fig. 2(c). Also plotted here is an analytical estimate of the corresponding relative emission probability [18], which is proportional to $[\mathrm{I}_m(\nu R/\upsilon\gamma)]^2$, where I_m is the modified Bessel function, γ is the Lorentz correction factor $(1 - \upsilon^2/c^2)^{-1}$, and R is the radial distance of the beam injection point from the axis of the well. The offset zero level seen in the experimental data is related to the imperfect cylindrical symmetry of the well.

This basic emission process bears some similarity with the Smith-Purcell effect [13], whereby a continuum of light wavelengths (varying with electron energy and the direction of emission) is generated as electrons pass over the surface of a planar metal grating. However, in the present case emission occurs via coupling to the 1D photonic bands of the periodically structured well so that discrete emission wavelengths are produced, determined by the condition that the wave vector of a guided mode is equal to ν/υ. This fundamental consideration is analyzed in Fig. 3, which shows the dispersion diagram for the guided electromagnetic modes of a cylindrical gold cavity with a radius of 350 nm, folded over the first Brillouin zone to account for a periodicity a of 400 nm in the direction parallel to the axis of the tube. Modes with azimuthal numbers $m = 0$, 1, and 2 are shown alongside the free-space light line and lines associated with electron energies of 20, 30, and 40 keV. (For the same reason that periodic patterns of subwavelength holes in a planar metal surface do not substantially change its properties, even at high filing-factors, except very close to the Brillouin zone boundaries [19], the presence of silica inclusions in the wall of the experimentally studied cavity will not significantly alter the mode structure except around $q = 0$ and π/a where some distortion will occur.) Electrons can couple to cavity modes where their respective lines intersect. This plot illustrates that the accessible mode profile is a complex function of electron energy, but one can immediately see that an electron of a given energy can couple to a number of modes at different energies (wavelengths) and that a given intersection point will shift to higher energies (shorter wavelengths) with increasing acceleration voltage, as observed experimentally.

The efficiency of the emission process has been evaluated in terms of the number of photons at the peak wavelengths generated per incident electron. (The number of photons being derived from a multiple Gaussian fit to the recorded spectra, taking into account the throughput efficiency of the light collection system; the corresponding

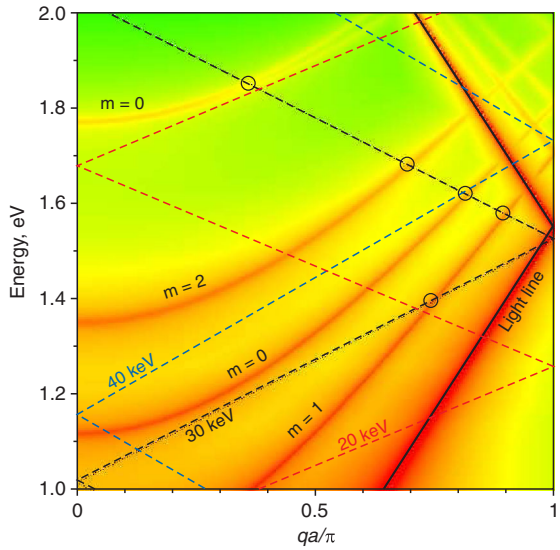

FIG. 3 (color online). Dispersion diagram showing the guided modes of an infinite periodic cylindrical gold cavity with a radius of 350 nm (azimuthal numbers $m = 0$, 1, and 2), superimposed with the free-space light line (solid black) and lines associated with electron energies of 20, 30, and 40 keV (dashed lines). Points of intersection between the 30 keV line and the cavity modes are circled.

number of electrons being given by the beam current and sampling time.) It is found to reach 1.9×10^{-5} for peak I and 3.4×10^{-5} for peak II at 40 keV, giving a light source with an output power of the order of 0.1 nW in either case; an emission intensity of $\sim 200\ \mathrm{W/cm^2}$.

To summarize, we provide the first proof-of-concept demonstration of a tunable, electron-beam-driven, nanoscale radiation source in which light is generated as free electrons travel down a light well—a nanohole through a stack of alternating metal and dielectric layers. Incoherent near-infrared emission is demonstrated in the present case but we believe that the concept may readily be scaled at least from the THz range to the UV domain by varying the periodicity of the structure (the Smith-Purcell mechanism has been experimentally demonstrated over this range [20,21]; constraints on electron beam quality approaching the Heisenberg uncertainty limit would seem to preclude extension to shorter x-ray wavelengths [22]). It is anticipated that longer wells will produce narrower emission lines, and that optimization of the light-well geometry, material composition and pumping regime will substantially improve emission efficiency. Indeed, if losses can be controlled (for example, by inhibiting surface plasmon generation and transverse light guiding) and higher (perhaps pulsed) drive currents are employed, it may be possible to achieve coherent, superradiant or even lasing emission modes [23–26]. The simplicity and nanoscale dimensions of the light-well geometry make it a potentially important device for future integrated nanophotonic circuit, optical memory and display applications where it may

be driven by the kinds of microscopic electron sources already developed for ultrahigh-frequency nanoelectronics and next-generation flat-panel displays [12].

The authors from the University of Southampton acknowledge the support of the UK Engineering and Physical Sciences Research Council (EPSRC, Projects No. EP/C511786/1 and No. EP/F012810/1) and the European Union (FP6 Project No. NMP4-2006-016881, ''SPANS''); Those from the National Taiwan University thank the National Science Council of Taiwan (NSC-97-2120-M-002-013, NSC-97-2112-M-002-023-MY2, and NSC-97-2915-I-002-001) and the EPSRC (EP/F012810/1); Professor García de Abajo acknowledges the European Union (NMP4-2006-016881) and the Spanish MEC (MAT2007-66050 and Consolider 'NanoLight.es').

*kfm@orc.soton.ac.uk; http://www.nanophotonics.org.uk/niz

[1] D. M. Koller, A. Hohenau, H. Ditlbacher, N. Galler, F. Reil, F. R. Aussenegg, A. Leitner, E. J. W. List, and J. R. Krenn, Nat. Photon. **2**, 684 (2008).
[2] M. T. Hill, Y.-S. Oei, B. Smalbrugge, Y. Zhu, T. de Vries, P. J. van Veldhoven, F. W. M. van Otten, T. J. Eijkemans, J. P. Turkiewicz, and H. de Waardt, Nat. Photon. **1**, 589 (2007).
[3] D. J. Bergman and M. I. Stockman, Phys. Rev. Lett. **90**, 027402 (2003).
[4] N. I. Zheludev, S. L. Prosvirnin, N. Papasimakis, and V. A. Fedotov, Nat. Photon. **2**, 351 (2008).
[5] H.-G. Park, C. J. Barrelet, Y. Wu, B. Tian, F. Qian, and C. M. Lieber, Nat. Photon. **2**, 622 (2008).
[6] S. Egusa, Y.-H. Liau, and N. F. Scherer, Appl. Phys. Lett. **84**, 1257 (2004).
[7] M. V. Bashevoy, F. Jonsson, A. V. Krasavin, N. I. Zheludev, Y. Chen, and M. I. Stockman, Nano Lett. **6**, 1113 (2006).
[8] J. T. van Wijngaarden, E. Verhagen, A. Polman, C. E. Ross, H. J. Lezec, and H. A. Atwater, Appl. Phys. Lett. **88**, 221111 (2006).
[9] M. V. Bashevoy, F. Jonsson, K. F. MacDonald, and N. I. Zheludev, Opt. Express **15**, 11 313 (2007).
[10] E. J. R. Vesseur, R. de Waele, M. Kuttge, and A. Polman, Nano Lett. **7**, 2843 (2007).
[11] J. Nelayah, M. Kociak, O. Stéphan, F. J. García de Abajo, M. Tencé, L. Henrard, D. Taverna, I. Pastoriza-Santos, L. M. Liz-Marzán, and C. Colliex, Nature Phys. **3**, 348 (2007).
[12] M. Nakamoto, in *IEEE Industry Applications Society Annual Meeting, Edmonton, Alberta, Canada* (IEEE, New York, 2008), pp. 447–451.
[13] S. J. Smith and E. M. Purcell, Phys. Rev. **92**, 1069 (1953).
[14] P. G. O'Shea and H. P. Freund, Science **292**, 1853 (2001).
[15] N. Yamamoto, K. Araya, A. Toda, and H. Sugiyama, Surf. Interface Anal. **31**, 79 (2001).
[16] H. Koyama, J. Appl. Phys. **51**, 2228 (1980).
[17] A. Mooradian, Phys. Rev. Lett. **22**, 185 (1969).
[18] F. J. García de Abajo, arXiv:0903.1669v1 [Rev. Mod. Phys. (to be published)].
[19] F. J. García de Abajo, Rev. Mod. Phys. **79**, 1267 (2007).
[20] J. Urata, M. Goldstein, M. F. Kimmitt, A. Naumov, C. Platt, and J. E. Walsh, Phys. Rev. Lett. **80**, 516 (1998).
[21] Y. Neo, H. Shimawaki, T. Matsumoto, and H. Mimura, in *Eighth IEEE International Vacuum Electronics Conference, Kitakyushu, Japan* (IEEE, New York, 2007), pp. 351–352.
[22] M. J. Moran, Phys. Rev. Lett. **69**, 2523 (1992).
[23] E. J. Reed, M. Soljačić, R. Gee, and J. D. Joannopoulos, Phys. Rev. Lett. **96**, 013904 (2006).
[24] A. Gover, Phys. Rev. ST Accel. Beams **8**, 030701 (2005).
[25] H. L. Andrews and C. A. Brau, Phys. Rev. ST Accel. Beams **7**, 070701 (2004).
[26] A. Bakhtyari, J. E. Walsh, and J. H. Brownell, Phys. Rev. E **65**, 066503 (2002).